A Miniature Force Sensor for Prosthetic Hands

Robert Platt, Mars Chu, Myron Diftler, Toby Martin, Michael Valvo

Dexterous Robotics Laboratory
Johnson Space Center, NASA
{robert.platt-1,mars.w.chu,myron.a.diftler,toby.b.martin,michael.c.valvo}@nasa.gov

Tactile sensing is an important part of the development of new prosthetic hands. A number of approaches to establishing an afferent pathway back to the patient for tactile information are becoming available including tactors and direct stimulation of the afferent nerves [1]. Tactile information can also be used by low-level control systems that perform simple tasks for the patient such as establishing a stable grasp and maintaining the grasping forces needed to hold an object. This abstract reports on the design of a small fingertip load cell based on semi-conductor strain gauges. Since this load cell is so small (measuring only 8.5mm in diameter and 6.25 mm in height), it easily fits into the tip of an anthropomorphic mechatronic hand. This load cell is tested by comparing a time series of force and moment data with reference data acquired from a much larger high-precision commercial load cell.

Several sensor technologies exist that have been applied to tactile sensing. One common technology is the force sensing resistor (FSR). These are made of a resistive polymer film that responds in a non-linear way to pressure. Another technology is quantum tunneling composite (QTC). When deformed, QTC material turns from a good insulator into a conductive material. Resistance drops exponentially as a function of pressure. Other force-sensing technologies are based on semiconductor strain-gauges. These have been used to measure pressure and to create multi-dimensional load cells. Multi-dimensional load cells are particularly good for tactile sensing because they can be very sensitive and they can be used to localize a contact point on a fingertip [2]. However, a drawback to using a load cell to sense forces in a robot hand has been size constraints: typical six-axis load cells are too large to fit into the tip or phalange of a human-sized robot finger.

The load cell proposed in this paper is comprised of three main components: a spring element, a strain gauge interface board, and an A/D electronics board. The sensor works by sensing loads applied to the outer shell shown in Figure 1. These loads are transmitted to through the spring element (the post in Figure 1) to the rest of the finger, the hand, and eventually to the ground. Six strain gauges are mounted on the spring element. The strain gauges are positioned so as to measure the six independent elements of strain. In order to protect the spring element, the outer shell was designed to make contact with the fingertip base under extreme loads. This secondary load path reduces the strain experienced by the spring element under these conditions.

Because of the small load cell size, electrical wire routing from the gauge down the finger and through the hand was
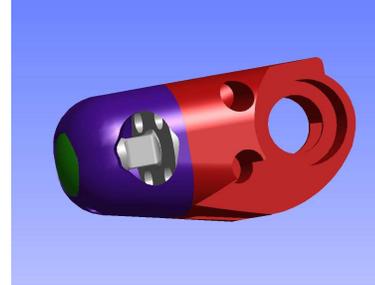
Fig. 1. Mechanical design of the outer shell (left), the spring element (middle), and the base of the fingertip load cell.

critical. The two wires from each strain gauge are routed to a strain gauge interface board, located at the base on the load cell. In the strain gauge interface board, each strain gauge is connected to a resistor bridge that converts the signal into a voltage. These signals are routed down the finger to the A/D electronics board. The A/D board is equipped to process data from up to five fingertip sensors. For each fingertip, the data from the six strain gauges is demultiplexed and converted to a digital signal. Finally, the signal is serialized into RS485 protocol and sent to the host computer.

In order to use the sensor, it is necessary to translate the output of the six strain gauges into a six-dimensional wrench. (Wrench is a three-dimensional force concatenated with a three-dimensional moment [3].) This is typically accomplished by multiplying the output of the strain gauge by a calibration matrix, K,

$$\mathbf{w} = K\mathbf{s}, \qquad (1)$$

where $\mathbf{s}$ is a six-dimensional vector of the strains and $\mathbf{w}$ is the equivalent wrench [4]. The calibration matrix was calculated by mounting the strain gauge on an off-the-shelf JR3 load cell and recording data from a number of sample loads. For each sample load, the output was recorded from the six strain gauges, $\mathbf{s}_i$, along with the wrench sensed by the JR3, $\mathbf{w}_i$. The calibration matrix, K, was calculated that most closely solved (minimized the least-squares error of) Equation 1 for all the sample loads. This was accomplished by accumulating the strain gauge vectors and wrench vectors into matrices, $W = (\mathbf{w}_1, \ldots, \mathbf{w}_n)$ and $S = (\mathbf{s}_1, \ldots, \mathbf{s}_n)$, using

$$K = WS^{\#}, \qquad (2)$$

where $S^{\#}$ is the pseudo-inverse of S,

$$S^{\#} = S^T(SS^T)^{-1}. \qquad (3)$$
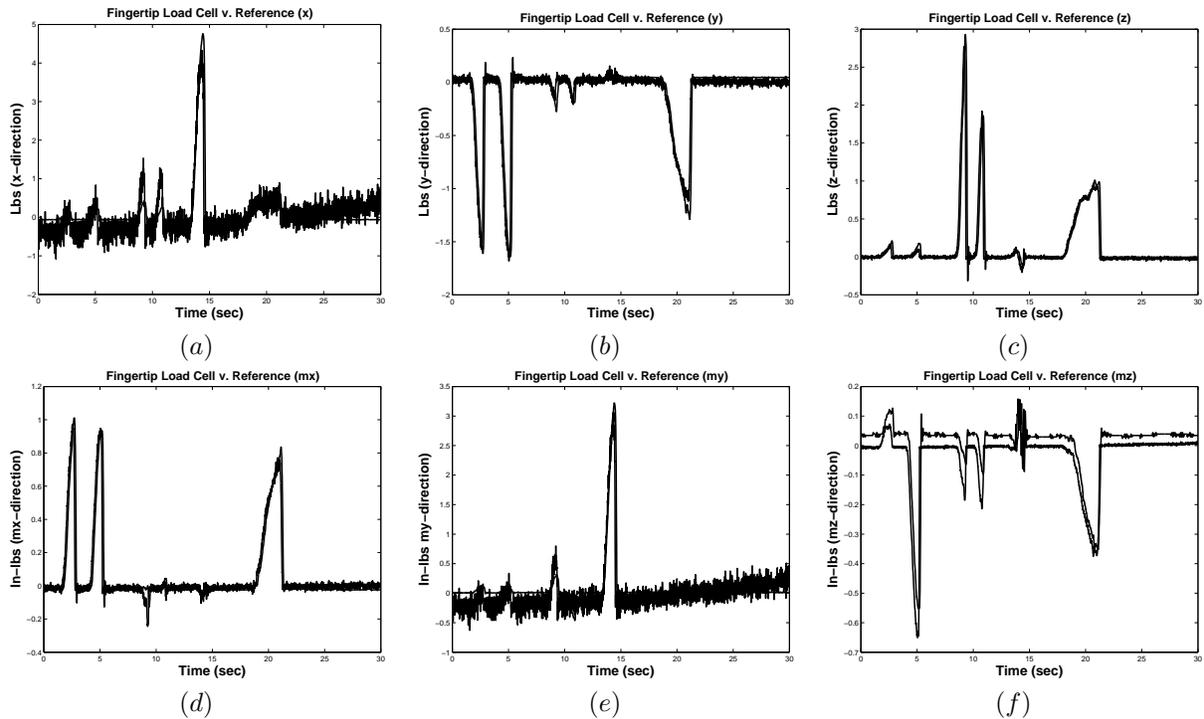
Fig. 2. The fidelity of the fingertip load cell compared with the output of a high-precision commercial load cell. Subfigures (a), (b), (c), (d), (e), and (f) make the comparison for the x, y, z force dimensions and the m_x, m_y, m_z dimensions, respectively.

K was calculated from a set of 18 sample loads.

After calibration, the fidelity of the calibration was tested by comparing the output of the new strain gauge (the result of Equation 1) with the output of the JR3. The results are illustrated in Figure 2. The six plots compare the output of the commercial load cell with that of the new load cell. The thick line shows the output of the commercial load cell while the thin line shows that of the new load cell. Each plot illustrates one of the six wrench dimensions. Note that, although the new load cell is significantly noisier in all six plots, the qualitative trend of the data is the same. Some dimensions are noisier than others. Note that the x and m_y dimensions (Figure 2(A) and (E)) are particularly noisy. This is a result of how the strain gauges are placed on the spring element. The configuration reflected in Figure 2 did not place any strain gauges on one side of the post-like spring element and was largely responsible for the noise evident in the m_y direction. Since collecting this data, the sensors have been redistributed so as to avoid this problem.

The noise in the x direction (Figure 2(a)) is a result of the shape of the spring element. The spring element deforms less in response to force in the x direction relative to other directions. Therefore, the strain gauges measure the less strain and, as a result, the calibration matrix is not conditioned well to measure this force. Also note the drift in the mean signal along the x and my directions. This is thermal drift caused by small changes in temperature in the spring element. Although all dimensions are subject to thermal drift, this problem is the worst along those dimensions that are not well conditioned.

Another reason for the noise and thermal drift is the small number of strain gauges. Because of size constraints, the design was only able to accommodate six strain gauges.

In conclusion, this abstract has presented a new miniature load cell designed to fit inside the fingertip of a humanoid finger. The load cell is comprised of six semiconductor strain gauges attached to a spring element that transmits loads from an outer shell to the rest of the finger. The fidelity of this sensor was tested and found to be more susceptible to noise compared to a high-precision commercial load cell, but a significant improvement over competing technologies for tactile sensing in humanoid fingers. Future work will attempt to improve the signal-to-noise ratio by adding more strain gauges and changing the shape of the spring element.

REFERENCES

[1] M. C. Carrozza, B. Massa, S. Micera, R. Lazzarini, M. Zecca, and P. Dario, "The development of a novel prosthetic hand – ongoing research and preliminary results," *IEEE ASME Transactions on Mechatronics*, vol. 7, no. 2, 2002.
[2] A. Bicchi, J. Salisbury, and D. Brock, "Contact sensing from force measurements," *International Journal of Robotics Research*, vol. 12, no. 3, 1993.
[3] R. Murray, Z. Li, and S. Sastry, *A Mathematical Introduction to Robotic Manipulation*. CRC Press, 1994.
[4] Y. Nakamura, *Advanced Robotics Redundancy and Optimization*. Addison-Wesley, 1991.